

**Accomplishment and Plan  
on AQUA Validation Science Research  
“Validation of AMSR Rainfall Using Airborne Precipitation Radar (PR-2)”  
RTOP # 291-07-72**

**Principal Investigator:** Eastwood Im (JPL)

**Co-Investigators:** Steve Durden (JPL), Li Li (JPL), Simone Tanelli (JPL)

**1. Research Objectives:**

The first research objective is to acquire the vertical profiling measurements of shallow rainfall and snowfall systems using the Second-generation Airborne Precipitation Radar (APR-2) aboard the NASA P-3 aircraft during the EOS AQUA AMSR validation field experiment in Wakasa Bay, Japan in Jan/Feb 2003, and to conduct the associated analysis in order to support the validation of the EOS AMSR-E instrument. Specifically we plan to:

- acquire dual-frequency, dual-polarization, Doppler data during field campaign;
- perform quality control and calibration;
- deliver the calibrated data set for archival;
- validate the retrieval capabilities of both EOS AQUA AMSR-E and ADEOS-II AMSR; and
- use the data to enhance our understanding of precipitation/snowfall processes.

The second research objective is to understand and quantify the Radio-Frequency Interference (RFI) problem associated with the 6.9-GHz brightness temperature measurements of AMSR.

**2. Second-generation Airborne Precipitation Radar (APR-2)**

The Second-generation Airborne Precipitation Radar (APR-2, Sadowy et al., 2003) is the airborne simulator of the next generation of the spaceborne rain mapping radars, which would follow the highly successful single-frequency Precipitation Radar (PR, Kozu et al., 2001) of the Tropical Rainfall Measuring Mission (TRMM, Kummerow et al., 2000). The APR-2 science observations will consist of vertical structures of rain reflectivity at both 13.4 and 35.6 GHz and at both co-polarization and cross-polarization, as well as the vertical Doppler measurements. Such comprehensive set of measurements from a highly mobile sensor is intended to provide information for the detailed studies of the microphysics and dynamics of rainfall, snowfall, and dense or precipitating clouds in various climatic regimes and geolocations.

The APR-2 operational geometry is shown in Figure 1; it looks downward and scans its dual-frequency antenna beams across the flight track, with each scan beginning at 25 degrees to the left of nadir and ending at 25 degrees to the right. The APR-2 scanning antenna consists of a 0.4-m offset reflector antenna with a mechanically scanned flat plate, and a 13.4- and 35.6-GHz dual-frequency antenna feed. The feed is configured such that the aperture at 35.6 GHz is under illuminated to provide matched beams at the two frequencies. The RF electronics subsystem consists of a digital chirp generator (DCG) used to synthesize a linear frequency-modulated chirp waveform, an upconverter and four receiver channels. The DCG generates the shaped, linearly frequency-modulated pulses with sidelobe levels below -60 dB. The chirp waveform is generated at an IF frequency and upconverted to both 13.4 GHz and 35.6 GHz. The signals are amplified to the desired radiated powers using the 13.4 and 35.6 GHz traveling wave tube amplifiers (TWTA) to the dual-frequency antenna. There are four receiver channels, two for 13.4 GHz (H- and V-pol) and two for 35.6 GHz (H- and V-pol). Table 1 shows the system characteristics for APR-2.

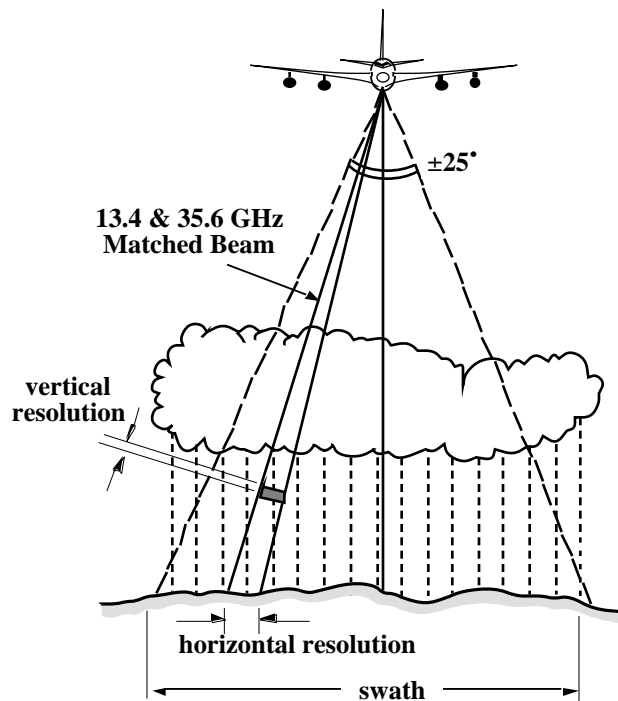


Figure 1: APR-2 operational geometry showing cross track scan.

Parameters	Ku-band	Ka-band
Frequency	13.4 GHz	35.6 GHz
Polarization	HH, HV	HH, HV
Antenna effective diameter	0.4 m	0.14 m
Antenna gain	34 dBi	34 dBi
Antenna sidelobe	-30 dB	-30 dB
Antenna scan angle	$\pm 25^\circ$	$\pm 25^\circ$
Polarization isolation	-25 dB	-25 dB
Peak power	200 W	100 W
Bandwidth	4 MHz	4 MHz
Pulsewidth	10 - 40 $\mu$ s	10 - 40 $\mu$ s
Pulse repetition frequency	5 kHz	5 kHz
Vertical resolution	37 m	37 m
Horizontal resolution (@ 9 km altitude)	600 m	600 m
Ground Swath	10 km	10 km
Sensitivity (@ 7 km range)	3 dBZ	3 dBZ
Doppler precision	0.3 m/s	0.9 m/s

Table 1: APR-2 system parameters.

At each beam position of each scan, APR-2 acquires simultaneous vertical profiling measurements of the following set of parameters:

- Co-polarized (HH) radar reflectivity at 13.4 GHz

- Cross-polarized (HV) radar reflectivity at 13.4 GHz
- Doppler velocity at 13.4 GHz
- Co-polarized (HH) radar reflectivity at 35.6 GHz
- Cross-polarized (HV) radar reflectivity at 35.6 GHz
- Doppler velocity at 35.6 GHz.

### 3. Wakasa Bay Experiment

The Wakasa Bay Experiment, conducted jointly by the U.S. AMSR-E and Japanese AMSR teams, is designed to: (1) validate the AMSR and AMSR-E shallow rainfall and snowfall retrieval capabilities; (2) extend the database of rainfall properties needed to implement a comprehensive physical validation scheme; and (3) extend our understanding of rainfall structures through the use of new remote sensing technology. The NASA contribution centers on the P3 aircraft carrying the Airborne Precipitation Radar (APR-2) operating at 14 and 35 GHz; an airborne cloud radar (ACR) operating at 94 GHz; a passive microwave sensor (PSR) that simulates the AMSR observations; a passive microwave radiometer (MIR) covering from 90 to 340 GHz; and an upward looking radiometer at 21 and 37 GHz (AMMR). The Japanese contribution consists of the GulfStream-II aircraft, a dual-polarized ground-based radar and its supporting observations. The combination allows the aircraft observations to cover a larger meteorological context.

The experiment was officially kicked off when the P3 aircraft arrived the Yokota Airforce Base near Tokyo, Japan on Jan 7, 2003. A total of twelve P3 flights were conducted between January 14 and February 3, 2003. The Wakasa Bay experiment log is listed in Table 2.

Flt #	Date	Flight/weather description	APR-2 data take
	1/7/03	P3 arrived Tokyo, Japan	
1	1/14/03	Snow over ocean	Yes
2	1/15/03	Snow over land	Yes
3	1/19/03	Oceanic shallow rain at low freezing level	Yes
4	1/21/03	Oceanic shallow rain at low freezing level	Yes
5	1/23/03	Widespread rain with cold front and squall line	Yes
6	1/26/03	Clear weather. 1 hr 35 min calibration flight for other P3 instrument.	No
7	1/27/03	First coordinated flight with Japanese GulfStream-II (GSII). Oceanic rainfall.	Yes
8	1/28/03	Coordinated flight w/ GSII. Scattered snow shower.	Yes
9	1/29/03	Coordinated flight w/ GSII. Widespread snow in Japanese Alps and Sea of Japan.	Yes
10	1/30/03	Coordinated flight w/ GSII. Cloud cover with embedded snow showers	Yes
11	2/1/03	Clear sky. Snow cover in Fukui, the calibration site.	Yes
12	2/3/03	Developing low with rain. P3 aircraft telemetry problem	Yes

Table 2: Wakasa Bay Experiment log.

## 4. APR-2 Data From Wakasa Bay Experiment

With the exception of a 1.5-hr clear-air calibration flight, APR-2 acquired dual-frequency rainfall and snowfall profiling measurements throughout the Wakasa Bay Experiment. As of the end of February 2003, the APR-2 reflectivity measurements have been preliminarily calibrated (approx 1 dBZ accuracy on Ku, 2 dBZ on Ka). Doppler velocity measurements were calibrated using surface reference and are in excellent agreement between the two frequencies. LDR measurements are referenced to the co-pol calibration, further analysis of the cross-pol channels is required to refine calibration. Two flight legs are shown here to illustrate the weather systems observed by APR-2.

### 4.1 Wide-spread Rainfall Observations by APR-2 (Figure 2)

Figure 2 shows the wide-spread rainfalls associated with the cold front and squall line that were observed by APR-2 on January 23, 2003. The nadir-track height profiles of co-polarized reflectivity, Doppler velocity, and Linear Depolarization Ratio (LDR) at both 13.4 GHz (Ku-band) and 35.6 GHz (Ka-band) are shown in this figure. The data represent the fourth flight line of the day, which is approximately 500 km long from E to W at 34° 30' N. With the exception of one instance, the P3 aircraft was kept at a steady altitude of 6.4 km with roll angles kept at less than 1°. In a 4-minute interval starting at 10:03 UTC, the aircraft made a 60° roll to allow PSR calibration and some small maneuvers to adjust the trajectory. Aircraft ground speed was between 120-130 m/s due to strong headwinds.

**09:47–10:01 UTC – Anvil.** A very stable bright band at about 2.4 km altitude (visible also in the LDR measures) separated the stratiform rain (with vertical velocity in the 5-7 m/s range) from the large ice crystals above (Ka reflectivity 3-5 dBZ lower than Ku reflectivity).

**10:06–10:20 UTC – Stratiform (light) rain bands.** A stable freezing level observed at 2.4 km altitude. Rain bands as thin as 500 m were visible throughout the interval. Ku and Ka radar backscatters were both in Rayleigh regime. Very little vertical air motion was observed.

**10:21-10:44 UTC – Stratiform (moderate) rain bands.** Freezing level slowly rose to 2.6 km. Ka reflectivity was significantly lower than the Ku reflectivity mainly due to attenuation. Large LDR values close to the surface were observed around 10:22 and 10:28. Further analysis is required for the correct interpretation of these signatures. Still, the measured vertical velocities did not reveal any vertical air motion.

**10:45–10:49 UTC – Cold front convection.** A light updraft was observed at 10:46, followed by a very strong rain cell (severe attenuation at Ka-band signals) with trailing downdraft. The large LDR at Ku-band suggests a possible mixing of rain and wet ice particles at the time. Supercooled water was observed at flight altitude.

### 4.2 Snowfall Observations by APR-2 (Figure 3)

Figure 3 shows the snowfalls measured by APR-2 in the first line of the 1/29/03 flight. The line is about 180 km long from south to north at 135° 30' E longitude. The P3 aircraft was kept at a steady altitude of 6.7 km with roll angles kept at less than 1°. Aircraft ground speed was ~180 m/s.

Five snow cells of varying intensity were observed. Some convection was observed in the first (03:19 UTC) and third cell (~03:24 UTC), otherwise, very small vertical velocities (0-3 m/s) were observed. The first three cells also showed higher cloud top (greater than 4km). Large particles caused Ka reflectivity to be several dB below Ku reflectivity. No LDR measurements are showed because the cross-polarized measurements fell below the sensitivity threshold of -30 dB as is expected from dry snow.

**Wakasa Bay Experiment – January 23rd 2003 – Flight 5 – Line 4**  
**From 34 30 N, 146 40 E (at 09:47) to 34 30 N 140 40 E (at 11:03)**

 TRMM pass

Jan 24, 2003 00:00

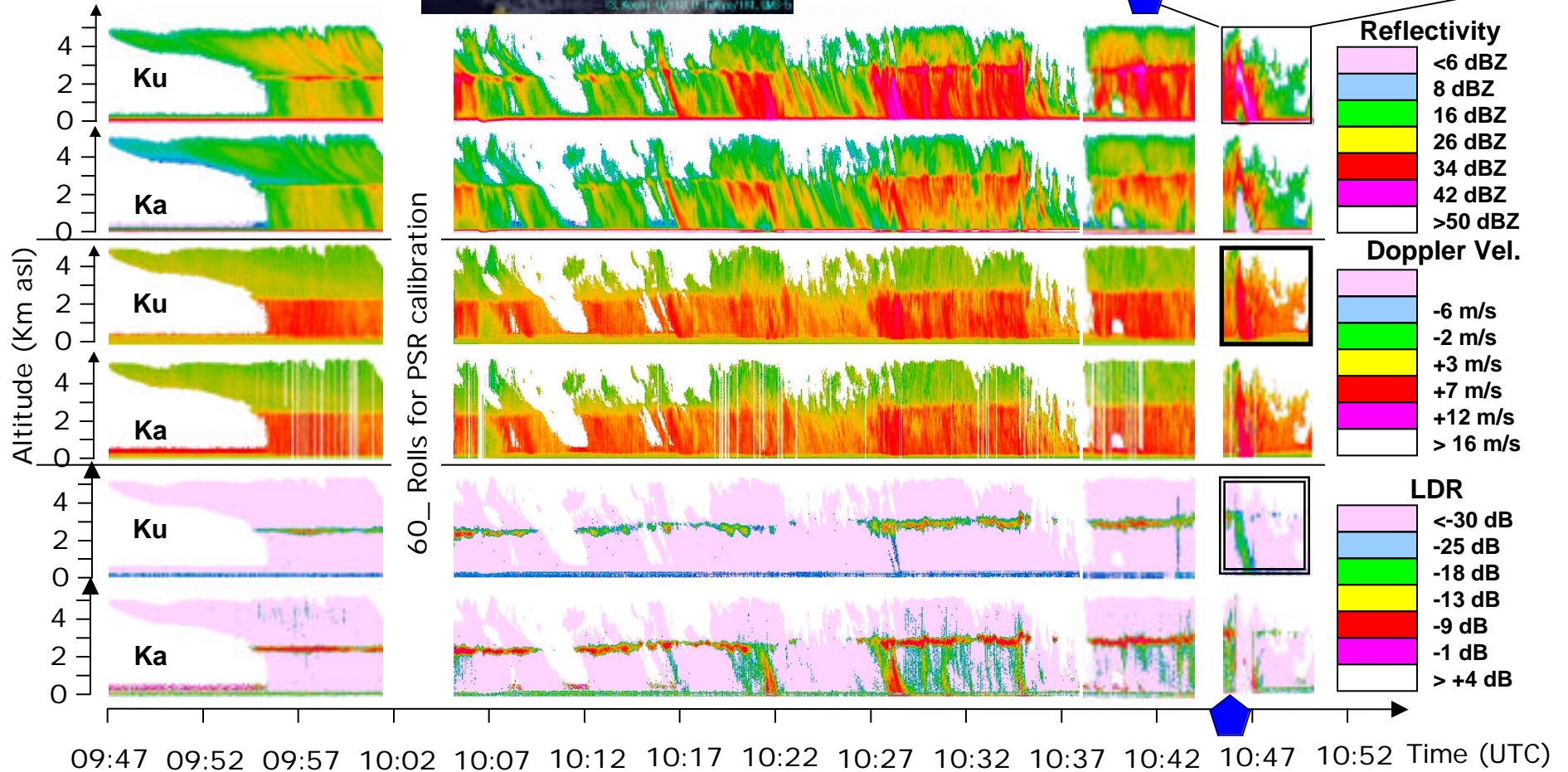
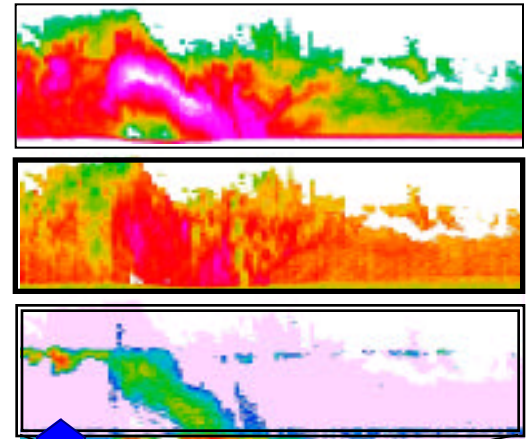
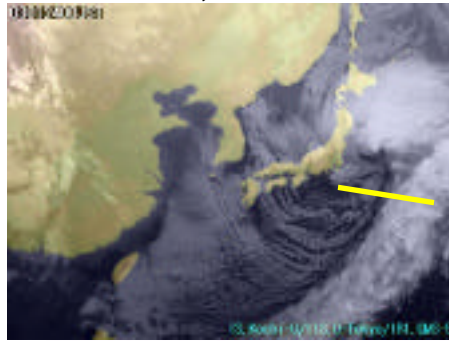


Figure 2: Wide-spread rainfalls observed by APR-2 on January 23, 2003.

**Wakasa Bay Experiment – January 29th 2003 – Flight 9 – Line 1**  
**From 36 30 N 135 30 E (at 03:16) to 38 30 N 135 30 E (at 03:39)**

Jan 29, 2003 02:00

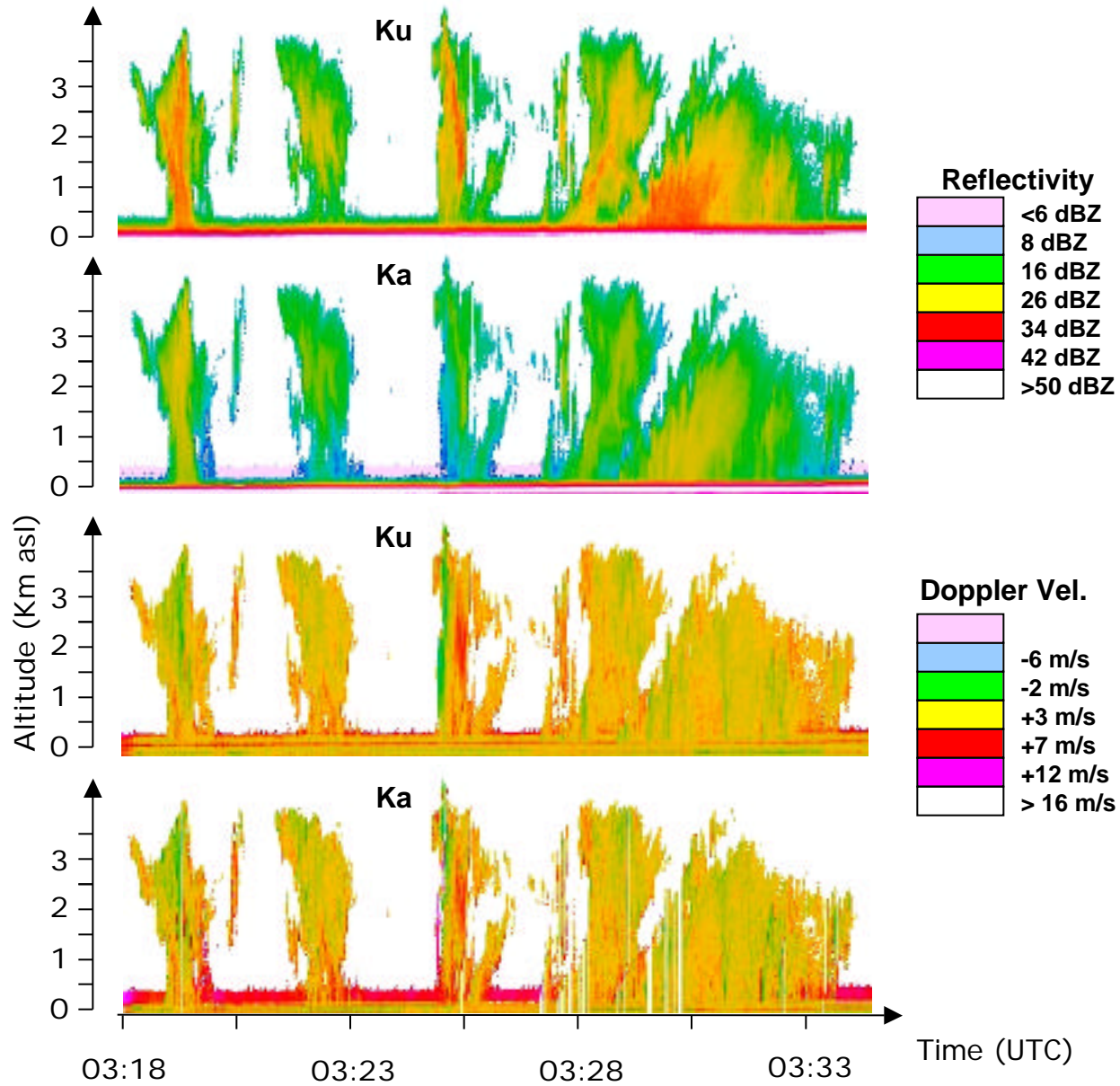
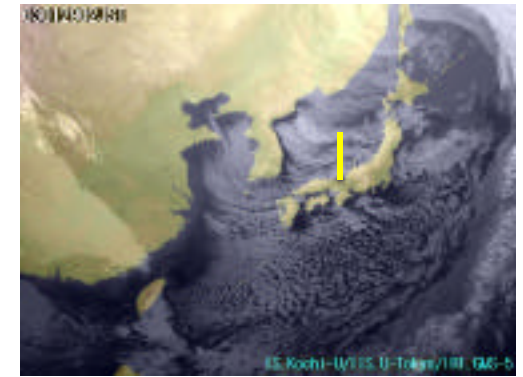


Figure 3: Wide-spread snowfalls observed by APR-2 on January 29, 2003.

## 5. Studies of AMSR-E RFI Over Land

Examination of the AMSR-E instrument science data have shown evidence of extensive Radio-Frequency Interference (RFI) in the 6.9-GHz brightness temperature (TB) measurements. Our early study indicated that this interference is best delineated by the negative spectral gradients between the measurements acquired at 6.9 and 10.7 GHz (i.e.,  $TB_{10.7} - TB_{6.9}$ ). We have subsequently developed a spectral gradient method, defined as RFI Index, to quantify the magnitude and extent of RFI observed over the U. S. in the Aqua AMSR-E 6.9-GHz radiometer channel.

A survey of RFI Index over North and Central America was generated by processing and merging multiple swaths of AMSR-E data for both vertical and horizontal polarization (Li, et al., 2003). The merged ascending pass swath data in vertical polarization for the U.S. are shown in Figure 4. Several distinct features are visible from the maps.

- In North and Central America, the RFI is confined mostly within the continental U.S. There is very little RFI in Canada and Mexico.
- The RFI occurs mostly at or near major U.S. cities or airports, with some exceptions. Some RFI can be distinguished along major highways. The possible RFI sources include, but are not limited to, facilities for cable TV relay, wireless communication, airport radar, and manufacturing operations, etc.
- Most RFI is close to being unpolarized, with some exceptions.
- The RFI intensities are stronger for ascending (near 1:30 pm) than for descending passes (near 1:30 a.m.), which may reflect differences in human activity patterns between day and night. Also, differences in RFI between ascending and descending passes may be due to differences in the AMSR-E antenna azimuth viewing direction of RFI sources.

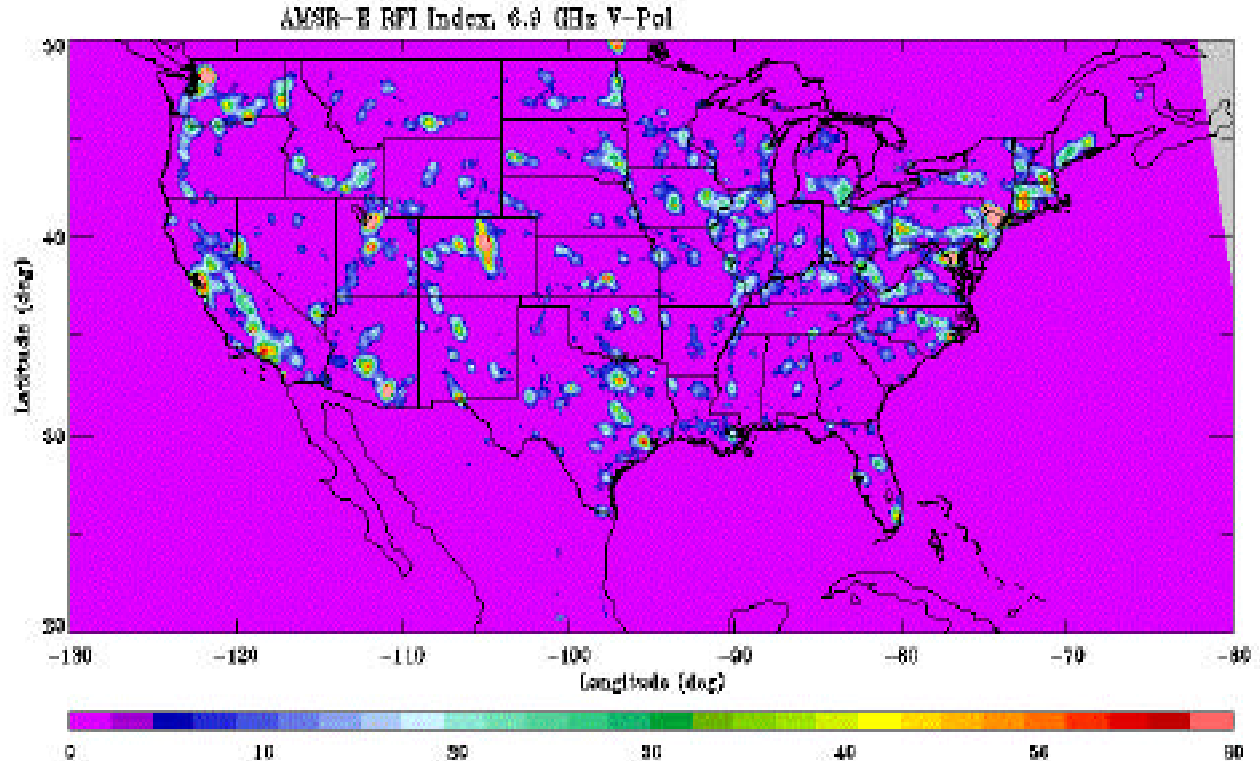


Figure 4: Vertically-polarized RFI index (RI) survey maps over the U. S. using AMSR-E ascending pass measurements.

More detailed regional maps were generated to focus on specific AMSR-E targets of interest, in particular the planned U.S. soil moisture validation sites. Figure 5 shows RFI maps for the regions of (a) Iowa, (b) Oklahoma, and (c) Alabama/Georgia. Cities with populations above 100,000 are indicated by asterisks. In Fig. 5a, there is widespread RFI evident in the neighborhoods of Des Moines, Cedar Rapids, and Sioux Falls, though not centered directly on those cities. Surprisingly there is no RFI near Madison and Lincoln despite the sizeable population and urbanization of these cities. Additional investigations need to be undertaken using ground-based RFI detectors to locate and characterize the specific sources of the RFI.

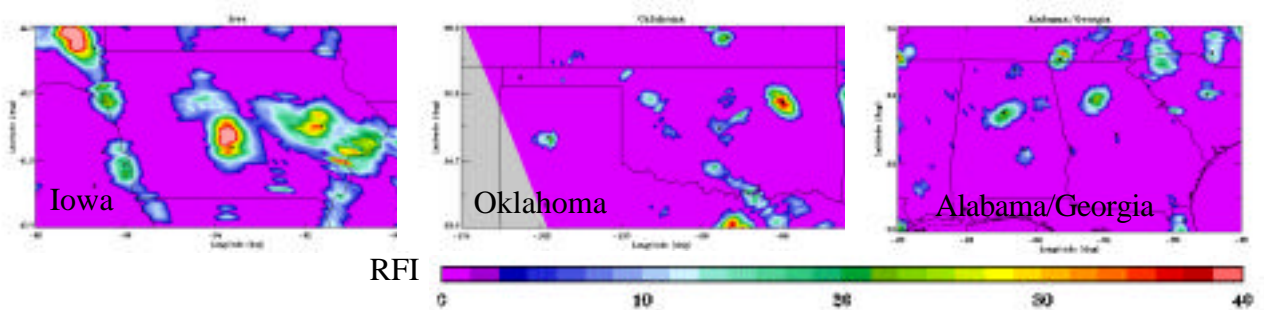


Figure 5: RFI index (RI) maps of regional areas in the U. S. centered in (a) Iowa, (b) Oklahoma, and (c) Alabama/Georgia.

## 6. Potential Use of RFI-Suppressed AMSR-E 6.9-GHz Data

In addition to identification and quantification of the RFI, we have also developed a preliminary RFI suppression technique to recover the corrupted C-band data. Our objective is to generate RFI suppressed brightness temperature (TB) data that are useful in land sensing applications. Figure 6a compares the in-situ soil moisture measurements against the AMSR-E soil moisture retrievals with the current algorithm that uses only the V- and H-polarization TB data at 10.6 and 18.7 GHz (4 channels). Figure 6b shows the same comparison but the retrieval here incorporates also the RFI-suppressed 6.9-GHz TB data at H- and V-polarizations (6 channels). The in-situ soil moisture data were obtained from the operational Soil Climate Analysis Network (SCAN) sponsored by USDA. The diagonal reference lines are used to indicate perfect match.

Figures 6a and 6b suggest that the RFI suppression technique as developed has the potential to improve the soil moisture retrievals. The rms difference between in-situ data and AMSR-E retrievals using the four-channel algorithm is  $0.1 \text{ g/cm}^3$ , and it improves to  $0.09 \text{ g/cm}^3$  with the six-channel algorithm. This represents about a 10% improvement. It is necessary to point out that the AMSR-E brightness temperatures used in this study have known calibration problems. So the accuracies provided here can be used in a relative terms only, and does not necessarily represent AMSR-E soil moisture retrieval accuracy.

## 7. Research Plan for Next 12 Months

- Perform post-experiment APR-2 data calibration
- Perform APR-2 data processing
- Conduct preliminary data analysis
- Study RFI sources
- Study RFI suppression and applications

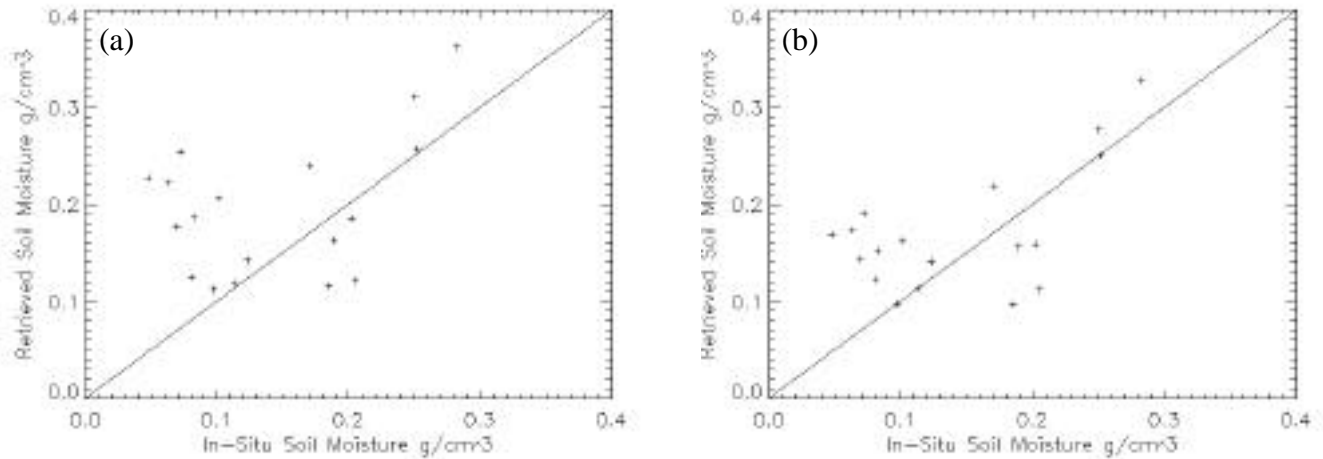


Figure 6: Comparison of in-situ vs. AMSR-E retrieved soil moisture measurements. AMSR-E retrievals use data from: (a) four channels (H- and V-polarization at 10.6 GHz and 18.7 GHz); (b) six channels (H- and V-polarization at 10.6 GHz, 18.7 GHz and RFI-suppressed 6.9 GHz).

## References

- Li, L., E. Njoku, E. Im, P. Chang, K. St.Germain, 2003: A Preliminary Survey of Radio-Frequency Interference over the U. S. in Aqua AMSR-E Data. *IEEE Trans. Geosci. Remote Sensing*. Submitted.
- Kozu, T., T. Kawanishi, H. Kuroiwa, M. Kojima, K. Oikawa, H. Kumagai, K. Okamoto, M. Okumura, H. Nakatsuka, and K. Nishikawa, 2001: Development of precipitation radar onboard the Tropical Rainfall Measuring Mission (TRMM) satellite. *IEEE Trans. Geosci. Remote Sensing*, **GE-39**, 102-43.
- Kummerow, C., J. Simpson, O. Thiele, W. Barnes, A.T.C. Chang, E. Stocker, R.F. Adler, A. Hou, R. Kakar, E. Wentz, P. Ashcroft, T. Kouz, Y. Hong, K. Okamoto, T. Iguchi, H. Kuroiwa, E. Im, Z. Haddad, G. Huffman, B. Ferrier, W.S. Olson, E. Zipser, E.A. Smith, T.T. Wilheit, G. North, T. Krishnamurti, and K. Nakamura, 2000: The status of the Tropical Rainfall Measuring Mission (TRMM) after 2 years in orbit. *J. Appl. Meteor.*, **39**, 1965-1982.
- Sadowy, G., A.C. Berkun, W. Chun, E. Im, and S.L. Durden, 2003: Development of an advanced airborne precipitation radar. *Microwave Journal*, 84-98.